Analytical Study of Collaborative Information Coverage for Object Detection in Sensor Networks

Guanqun Yang, Vinod Shukla, and Daji Qiao
Iowa State University, Ames, IA 50011
{gqyang, vkshukla, daji}@iastate.edu

Abstract—**Many sensor networks are deployed for the purpose of covering and monitoring a particular region, and detecting the object of interest in the region. In this paper, based on the probabilistic sensing model, we conduct comprehensive analytical and simulation studies on collaborative information coverage and object detection in wireless sensor networks. More specifically, we first define *point information coverage* and based on that we define ρ-*coverage* as a measure of the coverage performance for a randomly-deployed wireless sensor network. Then, we investigate the coverage and object detection performances of several simple decision fusion-based collaborative mechanisms and find that simple collaborations among active sensors indeed degrade the coverage performance due to the requirement of maintaining the target false detection probability. This motivates us to develop an on-demand collaborative framework for object detection, whose effectiveness is supported by detailed theoretical analysis and simulation-based validation. Finally, we investigate the energy efficiency performance of our proposed framework and identify the trade-offs among various system parameters in network power consumption.**

I. Introduction

Object detection is a major category of applications in wireless sensor networks. The goal of such an application is to determine whether the object of interest is present in the monitored region. Two sensing models have been widely used when investigating the object detection problem: the 0/1 disc sensing model [1]–[3] and the probabilistic sensing model [4]–[8]. Particularly, the latter one assumes that sensor measurements are affected by noise and the detection probability varies with the distance between the sensor and the object. Thus, two basic system metrics are considered: the probability of detecting an object and the probability of reporting a false detection. Based on the probabilistic sensing model, a number of research efforts [8]–[15] have been made to exploit the benefit of collaborative signal processing for object detection in wireless sensor networks. However, the corresponding coverage problem has not been well studied.

In this paper, based on the probabilistic sensing model, we define *point information coverage* and based on that we define ρ-*coverage* as a measure of the coverage performance for a randomly-deployed wireless sensor network. More specifically, a point t in the region is said to be information-covered if the detection probability of an object is no less than a pre-determined value $P_D^{\min}$ when the object is present at point t, while the system's false detection probability is no greater than a pre-determined value $P_{FD}^{\max}$. Accordingly, we say that the region is ρ-covered if at least ρ portion of all points in the region are information-covered. Throughout the paper, we analyze the coverage and object detection performances of various decision fusion-based [8] collaborative mechanisms for object detection in wireless sensor networks, and validate our analytical results with simulation.

The research reported in this paper was supported in part by the Information Infrastructure Institute (iCube) of Iowa State University, and the NSF under Grants No. CNS 0520102 and No. CNS 0716744.

Intuitively, collaboration among sensors is expected to produce better coverage than schemes without collaboration. However, upon detailed analytical study, we find that simple decision fusion-based collaborations among active sensors indeed degrade the coverage performance due to the requirement of maintaining the target false detection probability. This counterintuitive result motivates us to develop an on-demand collaborative framework for object detection.

The idea of our framework is that it no longer mandates active sensors to collaborate only with each other; instead, upon sensing a measurement higher than the decision threshold, an active sensor triggers its neighboring inactive sensors to collaboratively sense the environment. This way, by leveraging on the inactive sensors we could achieve the same low false detection probability while increasing the probability of detection because the density of inactive sensors is usually much higher than that of active sensors. The effectiveness of the proposed framework is supported by detailed theoretical analysis as well as simulation-based validation. Moreover, since decision fusion incurs extra energy consumption in aggregating collaborative messages, we further investigate the energy efficiency performance of the proposed framework, and offer some interesting observations and insights on how to select proper system parameters to maximize the network lifetime while maintaining the target coverage performance.

The rest of the paper is organized as follows. We discuss the related work in Section II. Then, we give system models and formulate the problem in Section III. Section IV studies several simple decision fusion-based collaborative mechanisms for object detection, and Section V provides the theoretical analysis of our proposed framework along with simulation-based validation. Energy efficiency performance of the proposed framework is studied in Section VI. Finally, we conclude the paper in Section VII.

II. Related Work

The coverage problem based on the 0/1 disc sensing model has been well studied [1], [16], [17]; in such model, an object inside (outside) a sensor's sensing disc is detected with probability one (zero). Despite its simplicity for analysis, many researchers consider alternative sensing models in order to better understand and characterize sensor measurements which are usually affected by noise and vary with the distance between the sensor and the object. Recent works [4]–[8], [18] assume the exposure model or the probabilistic sensing model to analyze coverage and detection problem in sensor networks.

978-1-4244-1777-3/08/$25.00 © IEEE
This full text paper was peer reviewed at the direction of IEEE Communications Society subject matter experts for publication in the IEEE SECON 2008 proceedings.

Collaboration among sensors [19]–[23] has been considered in many wireless sensor network applications such as estimation, localization, tracking and object detection. Particularly, in [24], the authors systematically investigate, define, design, and build a sensor network-based surveillance system, which uses collaborative signal processing to achieve better detection accuracy and noise rejection. Some fundamental problems on information fusion for distributed detection are studied in [8]–[12] where the local data or decisions of individual sensors are gathered by a fusion center to make the final decision. The performance of a distributed target detection system in the presence of faulty sensors, based on either value fusion or decision fusion, has been studied in [8], [12]. Although decision fusion may have lower detection accuracy (due to the compression of original information) compared with value fusion in some cases, it is more fault-tolerant and outperforms value fusion when the number of faulty sensors is large [8]. None of the above works considers the physical proximity between sensors and the object while in practice, as the signal emitted by the object decays fast with distance, readings by sensors far away from the object are less important to decision making.

In [5], the authors introduce the concept of virtual sensor resulting from neighboring sensors' collaboration based on value fusion, which may improve the coverage performance. In contrast to our work, [5] assumes that sensors' locations are known, so that a proper coverage set with less sensors can be derived by carefully choosing the nearby collaborating sensors. Due to the greedy and heuristic nature of their algorithm to find the coverage set, it is difficult to analyze the coverage performance of the resulting coverage set. In this paper, our proposed on-demand collaborative framework for object detection is based on decision fusion, and it does not require that each sensor is aware of its own location.

For the purpose of energy conservation, the concept of "on-demand" has been applied to many research areas in resource-constrained sensor networks such as data dissemination [25]. In [26], the authors develop energy-efficient protocols, called PECAS and MESH, that guarantee high quality of surveillance and conserve energy by operating sensors at proper states. Similarly, in [27], a sentry node may send power management packets to wake up non-sentry nodes to get more refined measurements when an event of interest is detected. In [28], the authors propose and design a new power management scheme using a radio-triggered hardware component to prolong the network lifetime. Equipped with a special radio-triggered circuit, a sleeping sensor (with both radio and CPU turned off) can be waken up by a special radio signal (in different frequency from regular data communications) from a nearby active sensor. While we use a similar "on-demand" idea in our proposed framework, the main contribution of this paper is to present comprehensive analytical and simulation studies of various collaborative mechanisms for object detection, including our proposed framework.

III. Models and Problem Formulation

A. System Model

We consider a sensor network consisting of $(N^a + N^i)$ wireless sensors randomly uniformly and independently deployed in a unit-area convex region $\mathcal{R}$, where N^a is the number of active sensors and N^i is the number of inactive sensors. Each active sensor senses at a certain sampling frequency f_s. We assume that sensors make object detection decisions based on snapshot readings. How to improve object detection by considering temporal correlation among sensor readings will be studied in the future work. We do not require sensors to be aware of their own locations.

In this paper, active sensors are called *sentry nodes* and inactive sensors are called *inert nodes*. There can be different models for the functioning of inert nodes. In one model, called *message-based model*, inert nodes are only listening but not performing any sensing task. A sentry node can trigger its nearby inert nodes to start performing the sensing tasks by flooding a message carrying the triggering command. In another model, called *circuit-based model*, inert nodes are sleeping and doing nothing. Under such a model, the sensors are provisioned with a special circuit for being triggered when need arises [28], and the triggering signal is transmitted at a different frequency channel from that being used for regular data communications. Sensors consume different levels of power at different states. $\mathcal{P}_{sentry}$ is the power consumed by sentry nodes. $\mathcal{P}_{trigger}$ is the power required to trigger an inert node and $\mathcal{P}_{inert}$ denotes the power consumed by inert nodes. Both $\mathcal{P}_{trigger}$ and $\mathcal{P}_{inert}$ vary with the inert node model.

B. Source Model

We study the objects which emit physical signals such as sound and electromagnetic waves. The strength of the signal emitted by the object decays according to power law, meaning that the signal strength measured at distance d away from the object is: [5], [8]

$$\omega = \begin{cases} \Omega, & d < d_0, \\ \frac{\Omega}{(d/d_0)^\alpha}, & d \geqslant d_0, \end{cases} \tag{1}$$

where Ω is the signal amplitude of the object, d_0 is a small constant, and α is a known decay exponent. Since our analysis below may be applied to any decay exponent, we let $\alpha = 2$ in this paper without loss of generality.

Assume that there is a single object in the region, which at any given time is either present or absent at a random location in the region according to certain probability distribution. Each active sensor collects its sensed reading of $\mathbf{x}$. Depending on the hypothesis of whether the object is present ($\mathcal{H}_1$) or not ($\mathcal{H}_0$), and the distance (d) between the object and the sensor if the object is present, sensed readings are:

$$\begin{aligned} \mathcal{H}_0 &: \mathbf{x} = n, \\ \mathcal{H}_1 &: \mathbf{x} = \omega + n, \end{aligned} \tag{2}$$

where ω is the received signal strength given by (1) and n is the background noise. In this paper, we use $F_N(n)$ to denote the cumulative distribution function of noise, and assume that it is identical and independent for all sensors.

C. Sensing and Alarm Models

In contrast to the 0/1 disc sensing model, we consider the probabilistic sensing model where (i) the sensor measurements are affected by noise; (ii) based on a pre-determined decision threshold, a sensor detects an object with a probability, which varies with distance between the sensor and the object. Assuming that a sensor is raising an alarm solely based on its own measurement ($\mathbf{x}$) and decision threshold (T), the probability of genuine alarm (p_a) and false alarm (p_{fa}) raised by the sensor are shown as areas of shaded regions in Figs. 1(a) and (b), respectively.

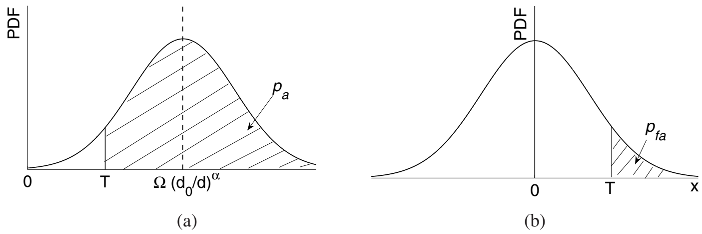

Fig. 1. (a) Probability of genuine alarm: $p_a = P(\mathbf{x} \geqslant T|\mathcal{H}_1)$ and (b) probability of false alarm: $p_{fa} = P(\mathbf{x} \geqslant T|\mathcal{H}_0) = 1 - F_N(T)$, where $\mathbf{x}$ is the sensor measurement, T is the decision threshold, and $F_N(\cdot)$ is the cumulative distribution function of noise.

D. Collaborative Information Coverage for Object Detection

There are two types of fusion algorithms for collaborative object detection [8] in wireless sensor networks: *value fusion* and *decision fusion*. In this paper, we investigate and analyze decision fusion-based collaborative object detection. That is, an object detection is claimed if at least K sensors out of a designated group (e.g., K sensors within certain distance from each other) report alarms where K is a design parameter. Value fusion-based collaborative object detection will be studied in the future work. We have the following definition.

DEFINITION 1 (Point Information Coverage): Given the decision fusion-based collaborative object detection described above, we say that a point t in the region is information-covered, if the detection probability of an object is no less than a pre-determined value ($P_D^{\min}$) when the object is present at point t, while the system's false detection probability is no greater than a pre-determined value ($P_{FD}^{\max}$).

Note that point information coverage is characterized by two probabilities $P_D^{\min}$ and $P_{FD}^{\max}$, which is inherently different from the conventional point coverage under the 0/1 disc sensing model. Moreover, due to random sensor deployment, full coverage of the region cannot be guaranteed and in some scenarios, full coverage may be too expensive or even unnecessary [17]. Instead, we study partial coverage of the region in this paper and have the following definition.

DEFINITION 2 (ρ-Coverage): Given the point information coverage defined above, we say that a region is ρ-covered, if at least ρ portion ($\rho \in (0,1)$) of all points in the region are information-covered.

When the size of the sensor network is sufficiently large (hence the edge effect may be neglected), and according to the above definitions of point information coverage and ρ-coverage, we have

$$\begin{aligned}\rho &= \iint_{\mathcal{R}} E\{I(x,y)\}dxdy \\ &= P(t \text{ is information-covered}) = P(P_D \geqslant P_D^{\min}),\end{aligned} \tag{3}$$

where t is an arbitrary point in the region $\mathcal{R}$ and

$$I(x,y) = \begin{cases} 1 & \text{point } (x,y) \text{ is information-covered,} \\ 0 & \text{otherwise.}\end{cases} \tag{4}$$

Our goal is to develop an energy-efficient collaborative mechanism to achieve ρ^*-coverage of the region, where the target ρ^* is given. Since it requires extensive statistical information (such as the pdf of P_D) to derive ρ directly, we apply Markov's inequality to ρ:

$$\begin{aligned}\rho &= P(P_D \geqslant P_D^{\min}) = 1 - P(P_D \leqslant P_D^{\min}) \\ &= 1 - P\left((1-P_D) \geqslant (1-P_D^{\min})\right) \\ &\geqslant 1 - \frac{E(1-P_D)}{1-P_D^{\min}} = 1 - \frac{1-E(P_D)}{1-P_D^{\min}} = \frac{E(P_D)-P_D^{\min}}{1-P_D^{\min}},\end{aligned} \tag{5}$$

and then study how to develop such a mechanism to make sure that (i) the system's false detection probability is no greater than $P_{FD}^{\max}$, and (ii) $E(P_D) \geqslant \rho^* + (1-\rho^*)P_D^{\min}$, which implies that the achieved ρ is always higher than the target ρ^* according to (5), while simultaneously maximizing the network lifetime. Note that we now only need information about $E(P_D)$ instead of its pdf.

IV. Problems with Simple Collaborative Mechanisms for Object Detection

We first investigate several simple decision fusion-based collaborative mechanisms for object detection.

A. A Naive Collaborative Mechanism

There are two types of object detection mechanisms in sensor networks: *without collaboration* and *with collaboration* among sensors. If without collaboration, a single sentry node reports a detection to the sink when its measurement is higher than the decision threshold. We use T_1 to denote the sentry node's decision threshold where subscript '1' indicates that the decision is solely based on its own measurement.

The first simple collaborative mechanism we investigate is a naive one based on [8] as follows. An object detection is reported if at least K sentry nodes sense a measurement higher than decision threshold T_K, where K is called the *collaboration degree*. Note that $T_K < T_1$ because, in order to maintain the same false detection probability, decision threshold decreases as K increases. The false detection probability P_{FD} can be calculated by:

$$P_{FD}(K, N^a) = 1 - \sum_{m=0}^{K-1} \binom{N^a}{m} (p_{fa})^m (1-p_{fa})^{N^a - m}, \tag{6}$$

where p_{fa} is the probability that an individual sensor raises a false alarm and equals $(1 - F_N(T_K))$, as shown in Fig. 1(b). Next, we calculate the expected detection probability $E(P_D)$, which will be denoted as $\bar{P}_D$ in the rest of this paper. To obtain $\bar{P}_D$, we first need to calculate $\bar{p}_a$, the probability that an individual sensor senses a reading higher than T_K, given that the object is present in the region. When the size of the sensor network is sufficiently large, we can neglect the edge effect and assume that the object is at center $(0,0)$ of the region $\mathcal{R}$ without loss of generality. Thus, $\bar{p}_a$ can be calculated by:

$$\bar{p}_a = \iint_{\mathcal{R}} \left(1 - F_N\left(T_K - \frac{\Omega d_0^2}{x^2+y^2}\right)\right) dxdy. \tag{7}$$

Because sensors are randomly independently distributed in the region and their readings are also independent from each other, we have

$$\bar{P}_D(K, N^a) = 1 - \sum_{m=0}^{K-1} \binom{N^a}{m} (\bar{p}_a)^m (1-\bar{p}_a)^{N^a - m}. \tag{8}$$

Now given the target false detection probability (P^*_{FD}), we observe through numerical studies that the expected detection probability ($\bar{P}_D$) goes down as the degree of collaboration (K) increases (as illustrated in Fig. 2). This is because, with a larger K, the increase in detection probability offered by a lower decision threshold (T_K) is offset by the decrease in detection probability due to a larger number of sentry nodes required to raise an alarm at the same time.

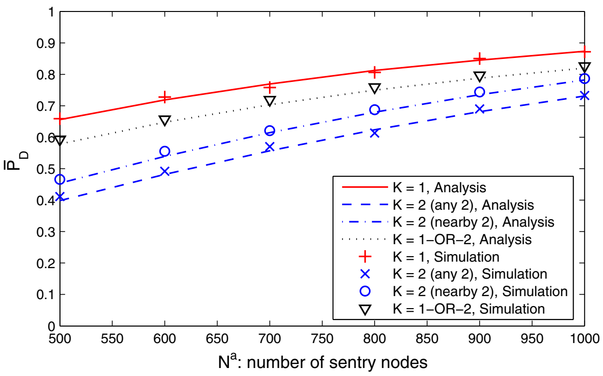

Fig. 2. Expected detection probability ($\bar{P}_D$) vs. number of sentry nodes (N^a) for various simple collaborative mechanisms. The target false detection probability is set to P^*_{FD} = 0.001. The dashed line for $K = 2$ shows the naive scheme where any K sentry nodes can collaborate while the dash-dotted line is for the enhanced version where only nearby sentry nodes are allowed to collaborate. The dotted line shows the 1-OR-2 collaborative scheme (with an arbitrary combination of T'_1 and T'_2).

B. An Enhancement to the Naive Collaborative Mechanism

In the above mechanism, since there is no constraint on which sentry nodes may collaborate, sentry nodes that are even far away from each other can collaborate to report a detection, thus resulting in a high P_{FD}. To improve upon this mechanism, we consider an enhancement as follows. Once a sentry node senses a reading higher than T_K,[1] it queries nearby active sensors within its neighborhood called *fusion range*, which is a circle with radius of R_f centered at the sentry node. Then, a detection is reported if and only if the sentry node receives at least $(K-1)$ alarms from active sensors within its fusion range. Accordingly, the system's false detection probability for this scheme can be calculated by:

$$P_{FD}(K, N^a) = 1 - (1 - \mathbb{P}_{FA})^{N^a}, \tag{9}$$

where $\mathbb{P}_{FA}$ is the probability that any sentry node reports a false detection after applying the localized decision fusion described above. Note that we treat distinct sentry nodes reporting false detections as independent events. This is reasonable because, due to the low false detection probability usually required by the system, sentry nodes that report false detection are likely far away from each other, hence their fusion ranges seldom overlap.

Next, we apply a general result from the theory of probability [29] to obtain $\mathbb{P}_{FA}$. According to the theory of probability, if the probability of an event A occurring in a single experiment is q, and if the number of independent experiments follows a Poisson distribution with parameter λ, the probability of event A occurring at least K times in the series of experiments is:

$$P = 1 - \sum_{m=0}^{K-1} e^{-q\lambda}\frac{(q\lambda)^m}{m!}. \tag{10}$$

When N^a is sufficiently large, the number of active sensors within the fusion range can be approximated by a Poisson distribution [30] with parameter $N^a\pi R_f^2$. Also, we know that the probability that a sensor raises a false alarm is p_{fa}. Thus, by applying the above general result from the theory of probability, we have:

$$\mathbb{P}_{FA} = p_{fa}\left(1 - \sum_{m=0}^{K-2}\frac{e^{-p_{fa}N^a\pi R_f^2}\left(p_{fa}N^a\pi R_f^2\right)^m}{m!}\right).$$

Substituting the above result about $\mathbb{P}_{FA}$ into (9), we complete the calculation of P_{FD}.

On the other hand, we know that, as long as there are at least K active sensors raising alarms within $\frac{R_f}{2}$ distance to the object, a detection will always be reported according to the localized decision fusion describe above. Let $\bar{\mathbb{P}}_A$ denote the expected probability that an active sensor, within $\frac{R_f}{2}$ to the object, raises an alarm; we have:

$$\bar{\mathbb{P}}_A = \int_0^{\frac{R_f}{2}} \frac{1}{\pi\left(\frac{R_f}{2}\right)^2}\cdot 2\pi r\cdot\left(1 - F_N\left(T_K - \frac{\Omega d_0^2}{r^2}\right)\right)dr. \tag{11}$$

Similarly, by applying the general result from the theory of probability, the expected detection probability $\bar{P}_D(K, N^a)$ is then given by:

$$\bar{P}_D(K, N^a) \geqslant 1 - \sum_{m=0}^{K-1}\frac{e^{-\bar{\mathbb{P}}_A N^a\pi\left(\frac{R_f}{2}\right)^2}\left(\bar{\mathbb{P}}_A N^a\pi\left(\frac{R_f}{2}\right)^2\right)^m}{m!}. \tag{12}$$

Though this enhancement improves upon the naive one still it gives inferior performance to the simple mechanism without collaboration (as shown in Fig. 2), regardless of the size of the fusion range (R_f). Fig. 2 plots the analytical and simulation results with R_f set to 0.1 units. To better understand the rationale, Fig. 3 shows the coverage region (according to our definition of point information coverage) of two neighboring active sensors in different scenarios. Comparing Fig. 3(a) with Figs. 3(b) and 3(c), we can see that the coverage region shrinks when two sensors collaborate with each other. In addition, we find that collaboration is beneficial only when two sensors are very close to each other.

At last, we study a 1-OR-2 collaborative scheme (K = 1 or 2) where an object detection is reported if at least one sentry node has sensed a reading higher than T'_1 or at least two sentry nodes have measurements larger than T'_2 ($T'_2 < T'_1$). The calculations of P_{FD} and $\bar{P}_D$ are similar to the analysis above, and the calculation details are omitted due to space limitation. Note that, due to the 'OR' operation, T'_1 and T'_2 are different from T_1 and T_2. Moreover, there is a fixed relation between T'_1 and T'_2 in order to achieve the target false detection probability. We exploit different combinations of T'_1 and T'_2 and through numerical studies, we observe that this scheme also yields worse performance than the simple scheme without

[1] For simplicity, we use the same notation T_K to represent the decision threshold for collaboration degree of K when we describe different collaborative mechanisms in Sections IV-A, IV-B, and V, though the actual value of T_K varies with the mechanism. This is because the group of K sensors participating in collaboration is different in different schemes. Similarly, we reuse the notations p_a, p_{fa}, $\mathbb{P}_{FA}$, $\bar{\mathbb{P}}_A$, P_{FD}, $\bar{P}_D$, and R_f.

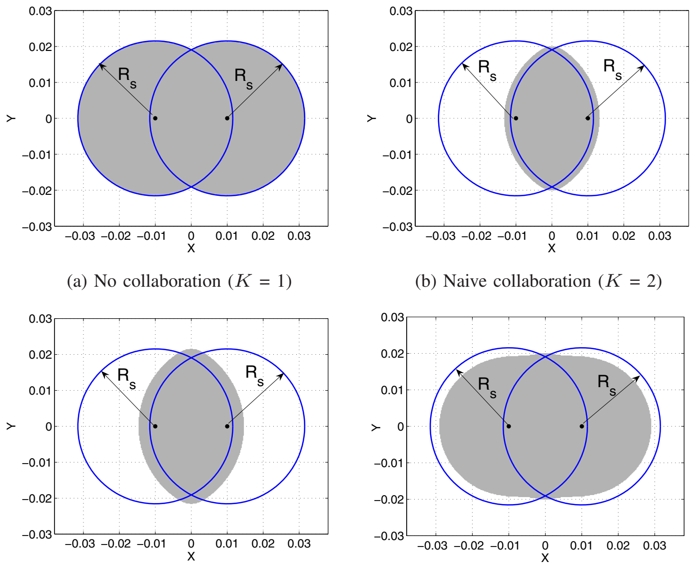

(a) No collaboration (K = 1)

(b) Naive collaboration (K = 2)

(c) Fusion range collaboration (K = 2)

(d) 1-OR-2 collaboration (K = 1 or 2)

Fig. 3. Coverage region (shown as shaded area) of two active sensors (apart by 0.02 units) in different collaboration scenarios. The detection thresholds used in the four scenarios result in the same P_{FD}. Note that the coverage regions in (b), (c) and (d) are smaller than that in (a).

collaboration (i.e., K = 1) regardless of the choices for T_1' and T_2'. This is because, the increase in detection probability by introducing collaboration is offset by the decrease in detection probability due to use of higher T_1' and T_2' to maintain the same target false detection probability. Fig. 2 plots the results with an arbitrary combination of T_1' and T_2' and Fig. 3(d) shows the coverage region of two neighboring sensors with the 1-OR-2 collaborative scheme. Similarly, performances of other combination schemes (e.g., 2-OR-3, 1-OR-2-OR-3, etc) are also worse than that of the simple scheme without collaboration.

C. Simulation-based Validation

The analytical studies in Sections IV-A and IV-B are validated by simulation results shown in Fig. 2. In the simulation, the object's source model is characterized by $\Omega = 2100$ mW and $d_0 = 0.001$ units, and the background noise follows a normal distribution $\mathcal{N}(0, \sigma^2)$ with $\sigma = \sqrt{2}$ mW. The target P_{FD}^* is 0.001. We test 100 different deployments. In each deployment, sensors are randomly deployed in a 1×1 unit area; we randomly select 100 locations for the object, and simulation is repeated 1000 times for each location. All simulation results match the analytical results very well.

Through above analytical and simulation studies, we note that the naive collaboration mechanism and its enhancements do not help improve the object detection performance. On the other hand, we suspect that better detection performance may be achieved if the collaboration among sensors is planned carefully. This motivates us to develop an on-demand framework for decision fusion-based collaborative object detection.

V. Analytical Study of the Proposed On-demand Collaborative Framework

A. Overview of the Proposed Framework

The key idea of our framework is that it no longer mandates sentry nodes to collaborate only with each other; instead it exploits the fact that, if a sentry node senses the object, its neighboring inert nodes may also be able to sense the object upon being triggered. This way, by leveraging on the inert nodes we could achieve the same low false detection probability while increasing the probability of detection because the density of inert nodes is usually much higher than that of sentry nodes. Next, we give a brief overview of our proposed on-demand collaborative framework, whose detailed description can be found in [31], and then focus on analysis of false detection probability and expected detection probability with the proposed framework.

We define two new concepts in our proposed framework: *detection zone* and *fusion range*. Detection zone (written as D.Z. in short) is defined as a disc centered at the object and with a radius of R_d. If the distance between a sensor and the object is larger than R_d, the probability of the sensor's measurement exceeding the decision threshold is less than a very small value (we use 1% in this paper) hence negligible. On the other hand, if a sensor is within R_d from the object, the probability of its measurement exceeding the decision threshold cannot be neglected and varies with the distance between the sensor and the object. Fusion range is defined as a disc centered at a sentry node and with a radius of $R_f = 2R_d$. Such definition of fusion range guarantees that, whenever a sentry node is within D.Z. of the object and senses a measurement above the decision threshold (which itself is a high-probability event), all inert nodes within D.Z. will be triggered.

In our proposed on-demand framework, upon sensing a measurement higher than the decision threshold (T_K), a sentry node triggers the neighboring inert nodes within its fusion range to collaboratively sense the environment. A collaboration degree of K means that, in order to report a detection of the object, a sentry node which initiates the detection process needs to receive at least $(K-1)$ positive alarms from sensors (sentry nodes or inert nodes) within its fusion range.

B. Theoretical Analysis

1) False Detection Probability: When there is no object in the monitored region, a sensor's reading is only affected by noise. The false detection probability P_{FD} is the probability that at least one sentry node reports a false detection:

$$P_{FD}(K, N_K^a, N_K^i) = P(\text{detection}|\mathcal{H}_0) = 1 - (1 - \mathbb{P}_{FA})^{N_K^a}, \quad (13)$$

where $\mathbb{P}_{FA}$ is the probability that a sentry node reports a false detection for a collaboration degree of K. N_K^a is the number of sentry nodes. Clearly, when $K = 1$, $\mathbb{P}_{FA} = p_{fa} = 1 - F_N(T_1)$, where T_1 is the corresponding decision threshold, as shown in Fig. 1(b). For $K > 1$, sensors collaborate and $\mathbb{P}_{FA}$ is given by:

$$\begin{aligned}\mathbb{P}_{FA} &= p_{fa} \cdot P(\text{at least } K-1 \text{ sensors within fusion range raise alarms}) \\ &= p_{fa} \cdot (1 - P_b),\end{aligned} \quad (14)$$

where

$$\begin{aligned}P_b &= P(\text{at most } K-2 \text{ sensors raise alarms}) \\ &= \sum_{m=0}^{N_K^i + N_K^a - 1} \frac{(\lambda \cdot \|D.Z.\|)^m \cdot e^{(-\lambda \cdot \|D.Z.\|)}}{m!} \times \\ &\quad \left(\sum_{n=0}^{\min(K-2,m)} \binom{m}{n} (p_{fa})^n (1-p_{fa})^{m-n} \right),\end{aligned} \quad (15)$$

where $\lambda = N_K^i + N_K^a$ is the node density. (15) is obtained based on the assumption that when the total number of sensors is large, the number of sensors in a sub-region follows a Poisson distribution [30]. Similar to previous analysis in Section IV-B, we make a reasonable assumption that distinct sentry nodes reporting false detections are independent events.

2) Expected Detection Probability: The calculations of $\bar{P}_D$ and P_{FD} are related since both vary with K, T_K, N_K^a and N_K^i. Next we describe the calculation details for $\bar{P}_D(K, N_K^a, N_K^i)$ when P_{FD} is given and equals the target P_{FD}^*. The probability of detection is the conditional probability that given the object is present, at least one sentry node reports a detection. Recall that the probability that a sentry node outside D.Z. recording a detection is very low. Therefore, we have:

$$\begin{aligned}
&\bar{P}_D(K, N_K^a, N_K^i) = P(\text{detection}|\mathcal{H}_1) \\
&\gtrapprox \sum_{n=K}^{N_K^a+N_K^i} P(\text{n sensors inside D.Z.}) \times \\
&\sum_{m=K}^{n} P(\text{m sensors raising alarms upon triggered by a sentry node inside D.Z.}) \\
&= \sum_{n=K}^{N_K^a+N_K^i} \frac{(\lambda \cdot \|D.Z.\|)^n . e^{(-\lambda \cdot \|D.Z.\|)}}{n!} \times \\
&\sum_{m=K}^{n} \left(\binom{n}{m} (\bar{\mathbb{P}}_A)^m (1-\bar{\mathbb{P}}_A)^{n-m} \right) \left(1 - \left(\frac{N_K^i}{N_K^a + N_K^i} \right)^m \right),
\end{aligned} \tag{16}$$

where $\lambda = N_K^a + N_K^i$ is the node density in the network. $\bar{\mathbb{P}}_A$ is the expected probability that a sensor within D.Z. has a measurement higher than T_K:

$$\bar{\mathbb{P}}_A = \int_0^{\frac{R_f}{2}} \frac{1}{\pi \left(\frac{R_f}{2}\right)^2} \cdot 2\pi r \cdot \left(1 - F_N \left(T_K - \frac{\Omega d_0^2}{r^2} \right) \right) dr. \tag{17}$$

C. Simulation-based Validation

In this section, we conduct numerical and simulation studies to support the above theoretical analysis. First, we study the performance of our proposed framework in terms of detection probability with respect to N_K^a, N_K^i, and T_K for various K. For a fixed $N_K^a + N_K^i$ (i.e., the total number of sensors deployed) and a target false detection probability $P_{FD}^* = 0.001$, Fig. 4 shows $\bar{P}_D$ for different K with respect to varying N_K^a. We observe that for a fixed N_K^a, $\bar{P}_D$ increases with K. $\bar{P}_D$ also increases with increase in N_K^a. However, for a fixed N_K^a, the performance improvement is not significant for higher degree of collaboration, e.g., K increasing from 3 to 4.

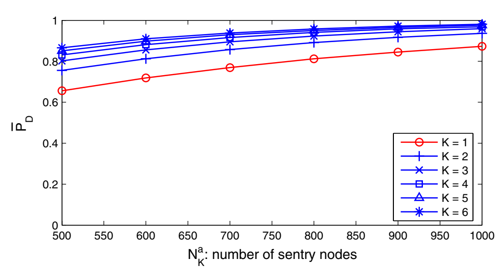

Fig. 4. Expected detection probability ($\bar{P}_D$) vs. number of sentry nodes (N_K^a) when $P_{FD}^* = 0.001$ and $N_K^a + N_K^i = 4000$.

We also study the variation of $\bar{P}_D$ with respect to varying N_K^i while keeping N_K^a fixed. The results are shown in Fig. 5. When N_K^i is low, we observe that the performance at a larger K is worse. This is as expected because having a smaller number of inert nodes implies that most of the sensors involved in collaboration will be sentry nodes. Consequently, the performance is similar to that observed in Section IV where collaboration is considered among sentry nodes only (see Fig. 2). However, as N_K^i increases, the performance for higher degree of collaboration increases because more inert nodes can participate in collaboration. Moreover, interested readers could refer to [31] to understand why the 'OR' collaborative schemes also do not perform well under our proposed framework.

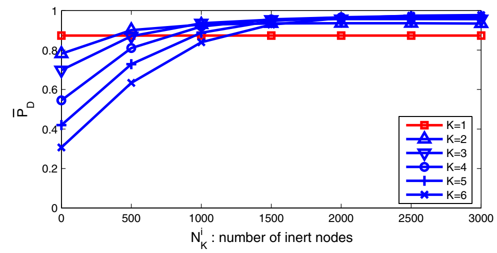

Fig. 5. Expected detection probability ($\bar{P}_D$) vs. number of inert nodes (N_K^i) when $P_{FD}^* = 0.001$ and $N_K^a = 1000$.

Fig. 6(a) shows the variation of decision threshold T_K (normalized with respect to Ω, signal amplitude of the object) and fusion range R_f with K for fixed P_{FD}, N_K^a and N_K^i. Corroborating our analysis, we observe that T_K decreases with increase in K, while R_f increases with increase in K. This means that, with a higher collaboration degree, each sentry node will have a larger detection zone, and therefore would trigger more inert nodes for collaboration.

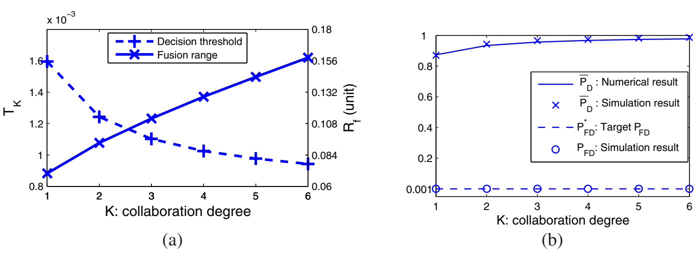

Fig. 6. (a) Normalized decision threshold (T_K) and fusion range (R_f) when $P_{FD} = 0.001$, $N_K^a = 1000$, and $N_K^i = 3000$. (b) Numerical and simulation results of $\bar{P}_D$ and P_{FD} when $P_{FD}^* = 0.001$, $N_K^a = 1000$, $N_K^i = 3000$, $\Omega = 2100$ mW, and $d_0 = 0.001$ units.

To verify the validity of our numerical analysis on $\bar{P}_D$ and P_{FD} we simulate our proposed framework with the following setup. First, the source model and the noise model are the same as those in Section IV-C. Then, we deploy 4000 nodes randomly in a unit area, out of which 1000 sentry nodes regularly sense the environment. We test 10 different deployments for evaluating the detection probability and false detection probability. For simulating the detection probability, we randomly choose 1000 different locations for the object and simulation is repeated 100 times for each object location. We evaluate the false detection probability based on 10000 trials. Results plotted in Fig. 6(b) show a close correspondence between our numerical and simulation results.

We also evaluate the coverage performance for different collaboration degrees and results are plotted in Fig. 7. We randomly deploy 4000 nodes in a unit area, and N_K^i and N_K^a are set to satisfy the following requirements: $P_{FD}^{\max} = 0.001$, $P_D^{\min} = 0.99$, and the target ρ^* is 90%. We test 10 different deployments. In each deployment, we randomly select 1000 different locations for the object, and simulation is repeated 100 times for each object location. As shown in the figure, the target ρ^* of 90% is achieved with all simulated collaboration degrees. The small discrepancy between the achieved coverage and ρ^* is due to application of the Markov's inequality in (5).

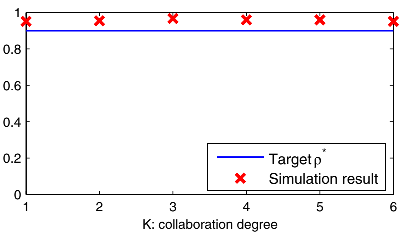

Fig. 7. Simulation results of coverage performance for different K, when $N_K^i + N_K^a = 4000$, $P_{FD}^{\max} = 0.001$, $P_D^{\min} = 0.99$, the target ρ^* is 90%, $\Omega = 2100$ mW, and $d_0 = 0.001$ units.

VI. Energy Efficiency Study of the Proposed On-demand Collaborative Framework

In this section we investigate the network energy efficiency performance when the proposed framework is adopted.

A. Design Objective

Let $\mathcal{P}(K, N_K^a, N_K^i)$ denote the power consumption for a wireless sensor network operating with our proposed framework, where K is the collaboration degree, N_K^a is the number of sentry nodes and N_K^i is the number of inert nodes. The objective is to find the optimal pair $(\hat{N}_K^a, \hat{N}_K^i)$ for a given K, which minimizes the network power consumption while guaranteeing a target ρ^*-coverage of the region. Here, we treat K as a given design preference, for example, when locating or tracking objects, a large K may be preferred for accurate results. In practice, if no preference is given for K, we could instead treat it as a tunable parameter in the design problem specified in (19); results for this case are omitted due to space limitation. However, based on our analysis, we can also find the optimal K^*, which can result in the lowest network power consumption among all K's. By using the results in Section III-D, the requirement of ρ^*-coverage can be translated into the requirements of P_{FD} and $\bar{P}_D$:

$$P_{FD}(K, N_K^a, N_K^i) \leqslant P_{FD}^* \text{ and } \bar{P}_D(K, N_K^a, N_K^i) \geqslant P_D^*, \tag{18}$$

where $P_{FD}^* = P_{FD}^{\max}$ and $P_D^* = \left(\rho^* + (1-\rho^*)P_D^{\min}\right)$. Recall that $P_{FD}^{\max}$ and $P_D^{\min}$ are the maximum false detection probability and the minimum detection probability which are used to define point information coverage and ρ-coverage in Section III-D. Formally, this design problem is stated as follows.

Given** K**,** P_{FD}^***, and** P_D^***, determine:

$$(\hat{N}_K^a, \hat{N}_K^i) = \arg \min_{\substack{P_{FD}(K,N_K^a,N_K^i) \leqslant P_{FD}^* \\ \bar{P}_D(K,N_K^a,N_K^i) \geqslant P_D^*}} \mathcal{P}(K, N_K^a, N_K^i). \tag{19}$$

Hence, $$\mathcal{P}^*(K) = \mathcal{P}(K, \hat{N}_K^a, \hat{N}_K^i). \tag{20}$$

The calculation of $\mathcal{P}(K, N_K^a, N_K^i)$ will be discussed in Section VI-C. In this paper, we only consider the power consumption for sensing, collaborative decision making and sensor's regular operation e.g. CPU and radio. The power consumed for a sentry node to report its detection to the sink is not considered as it varies with the routing and aggregation methods used. Once the methods are known, they can be incorporated into our power consumption analysis without much difficulty.

B. Observations and Simplification

The problem stated above is very complex and here we present some interesting observations that help simplify the problem.

- For a given collaboration degree K, let $\tilde{N}_K^a$ denote the minimum number of sentry nodes required to meet the system probability constraints. Therefore,

$$\tilde{N}_K^a = \arg \min_{\substack{P_{FD}(K,N_K^a,N_K^i) \leqslant P_{FD}^* \\ \bar{P}_D(K,N_K^a,N_K^i) \geqslant P_D^*}} N_K^a, \quad \forall K \geqslant 1. \tag{21}$$

- For a given collaboration degree K and number of sentry nodes $N_K^a \geqslant \tilde{N}_K^a$, let $\check{N}_K^i$ denote the minimum number of inert nodes required to meet the system probability constraints. Therefore,

$$\begin{aligned} &\textbf{\textit{Given }} K \text{ and } N_K^a, \ \textbf{\textit{where }} K \geqslant 1 \text{ and } N_K^a \geqslant \tilde{N}_K^a, \\ &\check{N}_K^i(N_K^a) = \arg \min_{\substack{P_{FD}(K,N_K^a,N_K^i) \leqslant P_{FD}^* \\ \bar{P}_D(K,N_K^a,N_K^i) \geqslant P_D^*}} N_K^i \\ &\qquad\qquad = \arg \min_{\substack{P_{FD}(K,N_K^a,N_K^i) \leqslant P_{FD}^* \\ \bar{P}_D(K,N_K^a,N_K^i) \geqslant P_D^*}} \mathcal{P}(K, N_K^a, N_K^i). \end{aligned} \tag{22}$$

The second equality in (22) is based on the fact that given the number of sentry nodes and collaboration degree, less inert nodes result in lower network power consumption. Further, when $N_K^a = \hat{N}_K^a$, $\check{N}_K^i(\hat{N}_K^a) = \hat{N}_K^i$.

With the help of above observations we are able to simplify our design problem and make the search space for optimal $(\hat{N}_K^a, \hat{N}_K^i)$ significantly smaller. The original problem given by (19) can now be restated as:

$$(\hat{N}_K^a, \hat{N}_K^i) = \arg \min_{\substack{N_K^a \geqslant \tilde{N}_K^a \\ N_K^i = \check{N}_K^i(N_K^a)}} \mathcal{P}(K, N_K^a, N_K^i). \tag{23}$$

C. Calculation of $\mathcal{P}(K, N_K^a, N_K^i)$

In Table I, we summarize the notations to be used in Sections VI-C and VI-D. Please note that $\mathcal{P}_{sentry}$ is equal to $(\mathcal{P}_{sense} + \mathcal{P}_{active})$, while $P_{inert} = \mathcal{P}_{active}$ for message-based inert node model and $P_{inert} = \mathcal{P}_{sleep}$ for circuit-based inert node model. For the message-based inert node model, the power consumption for the network can be easily derived as:

$$\mathcal{P}(K, N_K^a, N_K^i) = \begin{cases} \mathcal{P}_{sentry} N_1^a, & K = 1, \\ \mathcal{P}_{sentry} N_K^a + \mathcal{P}_{inert} N_K^i + \\ (\ (1 - P(\mathcal{H}_1))(1 - F_N(T_K)) + \\ \quad P(\mathcal{H}_1) P_n \bar{\mathbb{P}}_A + \\ \quad P(\mathcal{H}_1)(1 - P_n)(1 - F_N(T_K))\ ) \times \\ \quad N_K^a \left(E_f(K) + N_K^i R_f^2 \pi \mathcal{P}_{sense} \tau \right) f_s, & K > 1. \end{cases} \tag{24}$$

For the circuit-based inert node model, the power consumption can be calculated by (24) after the calculation of $E_f(K)$ is properly adjusted. Since the inert nodes are already awake in the message-based model, no energy is required to wake them up and $E_f(K)$ is simply the energy required for decision fusions. However, in the circuit-based model, in addition to the energy consumed for decision fusions, the sentry nodes consume extra energy for triggering the inert nodes within its fusion range [28].

D. Numerical Study and Simulation-based Validation

First, through numerical studies we offer some interesting insights on how the network energy efficiency performance varies with the inert node model, the collaboration degree and various parameters discussed in Sections V and VI. Table II lists the system parameters used for this study. Using these parameters, for $K = 1$ we obtain $\hat{N}_1^a = 1114$ and the corresponding power consumption $\mathcal{P}^*(1)$ is 3.453×10^5 mW. In the remaining of this section, all power consumptions are normalized over $\mathcal{P}^*(1)$. The solution to the optimization problem defined in Eq. (23) determines the optimal pair $(\hat{N}_K^a, \hat{N}_K^i)$ for a given K. Particularly, Fig. 8(a) shows the variation of network power consumption, when K is 5, with the number of sentry nodes varying from $\tilde{N}_5^a$ to $\hat{N}_1^a$. The results are shown for a fixed ratio of $\mathcal{P}_{sense}/\mathcal{P}_{active} = 4$ ($\mathcal{P}_{sense}$ = 248 mW, $\mathcal{P}_{active}$ = 62 mW). We see that, for the message-based inert node model, $\hat{N}_5^a = 655$ yields the lowest network power consumption of $\mathcal{P}^*(5) = 0.936$, and the corresponding $\hat{N}_5^i$ is 1800. Further, we see that $\tilde{N}_5^a = 620 < 655 = \hat{N}_5^a$. This is because when N_K^a decreases, N_K^i increases to satisfy the system probability constraints; since inert nodes consume a considerable amount of power in the message-based inert node model, a smaller N_K^a may not necessarily result in lower network power consumption.

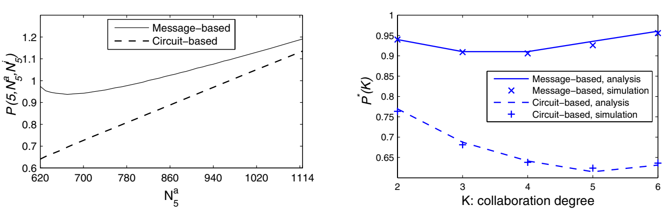

(a) (b)

Fig. 8. (a) Given $K = 5$, normalized network power consumption ($\mathcal{P}(5, N_5^a, N_5^i)$) vs. number of sentry nodes (N_5^a), with N_5^a varying from 620 ($\tilde{N}_5^a$) to 1114 ($\hat{N}_1^a$) and the corresponding N_5^i is equal to $\check{N}_5^i(N_5^a)$. (b) Normalized optimal network power consumption $\mathcal{P}^*(K)$ for different K and inert node models.

TABLE I
NOTATIONS FOR CALCULATING NETWORK POWER CONSUMPTION

Notation	Remarks
$\mathcal{P}_{sense}$	Power consumption for sensing task by each sensor.
$\mathcal{P}_{active}$	Power consumption, except sensing, for each active sensor.
$\mathcal{P}_{sleep}$	Power consumption for a sensor in sleeping state.
f_s	Sensing frequency for sentry node.
$E_f(K)$	Average energy consumption for executing one triggering process.
E_{msg}	Energy consumption for transmitting one message.
$P(\mathcal{H}_1)$	Probability that object is present in the network.
P_n	Probability that a sentry node is in D.Z. $P_n = (R_f/2)^2\pi$.
$\bar{\mathbb{P}}_A$	Prob. that a sensor in D.Z. has measurement $> T_K$. See Eq. (17).
τ	Time required to acquire a single sensor reading.

TABLE II
SYSTEM PARAMETERS USED IN NUMERICAL AND SIMULATION STUDIES

Parameter	Value	Remarks
Ω	2100 mW	Signal amplitude of the object.
d_0	0.001 unit	Constant in Eq. (1).
Noise	-	$\mathcal{N}(0, \sigma^2)$ where $\sigma = \sqrt{2}$ mW.
f_s	1 Hz	Sensing frequency for sentry node.
E_{msg}	2.23 mJ	Energy consumed to transmit one message.
$P(\mathcal{H}_1)$	0.9	Probability that object is present.
τ	30 ms	Time required to acquire a single sensor reading.

However, for the circuit-based inert node model, we find the lowest power consumption is achieved when $\hat{N}_5^a = \tilde{N}_5^a$ and, interestingly, the power consumption increases almost linearly with N_5^a, which is totally different from that for the message-based model. This is because, although a lower N_5^a requires a larger N_5^i, sleeping inert nodes consume much less power than sentry nodes. So, using the smallest number of sentry nodes always yields the lowest network power consumption. The results for other collaboration degrees are similar with the above case.

We further simulate the optimal power consumption under various collaboration degrees for validation purpose. We simulate 10 different deployments, where $N_K^a = \hat{N}_K^a$ and $N_K^i = \hat{N}_K^i$ for each K. We simulate the message-based and circuit-based models for 1000 sensing cycles each with $P(\mathcal{H}_1) = 0.9$. Simulation results are normalized and plotted in Fig. 8(b), which are very close to the analytical results.

Although we leave the decision of choosing a proper K to the system designer, to give an insight on how K affects the optimal power consumption in our proposed framework, we conduct a numerical study of network power consumption with variation in the ratio $\mathcal{P}_{sense}/\mathcal{P}_{active}$ for various K. Figs. 9 (a) and (b) show the trends for message-based and circuit-based inert node models respectively. Suppose the collaboration degree yielding the lowest power consumption is K^*. It is observed that K^* varies with the ratio $\mathcal{P}_{sense}/\mathcal{P}_{active}$. For the message-based model, if the ratio is below 1, we find that K^* is always 1 because inert nodes consume a considerable amount of energy for regular operation. However, when the ratio goes beyond 2, schemes with higher degree of collaboration start performing comparably to or even better than the non-collaboration scheme. This happens because the power consumption for regular sensing becomes dominant and schemes with higher degree of collaboration are able to work with a smaller number of sentry nodes compared to the non-collaboration scheme. This also explains why when the ratio is large enough, optimal network power consumption for different K is almost proportional to $\tilde{N}_K^a$ (see Table III).

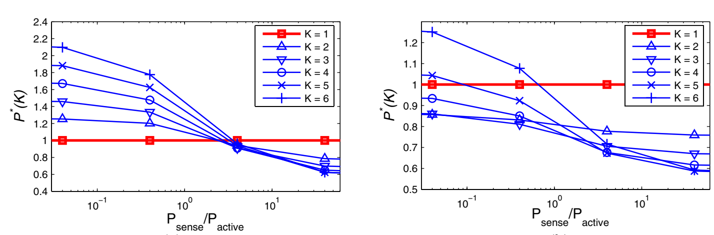

(a) (b)

Fig. 9. Normalized optimal network power consumption $\mathcal{P}^*(K)$ vs. $\mathcal{P}_{sense}/\mathcal{P}_{active}$ for (a) message-based and (b) circuit-based inert node model.

TABLE III
$\mathcal{P}^*(K)$ AND $\tilde{N}_K^a$ FOR VARIOUS K WHEN $\frac{\mathcal{P}_{sense}}{\mathcal{P}_{active}} = 40$

K	1	2	3	4	5	6
$\tilde{N}_K^a$	1114	840	735	665	620	610
$\mathcal{P}^*(K)$	1	0.7594	0.6684	0.6125	0.5806	0.5803

For the circuit-based model, we also find that, in general, the network power consumption for collaborative schemes ($K > 1$) decreases with the ratio $\mathcal{P}_{sense}/\mathcal{P}_{active}$. However, since the time required to trigger an inert node with respect to distance increases according to power law, sentry nodes consume much more energy for triggering the inert nodes than that for sensing and operation when the fusion range is large. As higher degree of collaboration usually results in a larger fusion range, this makes the overall network power consumption very large. In Fig. 9(b), we can see that for our setup, when the ratio $\mathcal{P}_{sense}/\mathcal{P}_{active}$ is low, power consumption for high-degree collaborations $K = 4, 5, 6$ is even higher than that for $K = 3$. However, when the ratio is large enough, the sensing power becomes the dominant factor and the curves follow the same trend as for the message-based model.

We also conduct numerical and simulation studies for different $P(\mathcal{H}_1)$ but the results do not vary much. This seems counterintuitive at the first sight but can be explained as follows. Since we consider the presence of only one object in the network and due to the low $P_{FD}^{\max}$ in our setup, D.Z. of an object is very small compared to the network size. So the portion of sensors affected by presence of an object is only a very small fraction and hence, the contribution of $P(\mathcal{H}_1)$ to the network power consumption is small. Please note that this observation does not always hold; e.g., when the network size is small, the impact of $P(\mathcal{H}_1)$ may be more significant.

E. Summary

We summarize the key observations for the proposed on-demand collaborative framework as follows.

- The circuit-based inert node model usually renders better network energy efficiency than the message-based model.
- For a given K, the smallest number of sentry nodes and inert nodes required to guarantee ρ^*-coverage may not result in the lowest network power consumption.
- With both inert node models, higher K does not always yield lower network power consumption.
- Collaboration among sensors is preferred when $\mathcal{P}_{sense}$ is high compared to $\mathcal{P}_{active}$.

VII. Conclusions

In this paper, we conduct analytical and simulation studies on information coverage and object detection performances of several decision fusion-based collaborative mechanisms in wireless sensor networks, including our proposed on-demand collaborative framework. Our studies are based on the probabilistic sensing model, and a point is said to be information-covered if and only if the detection probability is no less than $P_D^{\min}$ when the object is present at that point, and the system's false detection probability is no greater than $P_{FD}^{\max}$. We first investigate a few simple collaborative mechanisms for object detection and discover that simple collaborations among active sensors in fact degrade the coverage performance. This motivates us to design an on-demand collaborative framework, where inactive sensors can be triggered by nearby active sensors to collaboratively sense the object. The effectiveness of our proposed framework and its energy efficiency performance are analyzed and validated by simulation.

References

[1] X. Bai, S. Kuma, D. Xua, Z. Yun, and T. H. Lai, "Deploying Wireless Sensors to Achieve Both Coverage and Connectivity," *in Proc. ACM MobiHoc*, May 2006.
[2] Q. Cao, T. Yan, J. Stankovic, and T. Abdelzaher, "Analysis of Target Detection Performance for Wireless Sensor Networks," *in Proc. IEEE/ACM DCOSS*, June 2005.
[3] O. Dousse, C. Tavoularis, and P. Thiran, "Delay of Intrusion Detection in Wireless Sensor Networks," *in Proc. ACM Mobihoc*, may 2006.
[4] B. Liu and D. Towsley, "A Study of the Coverage of Large-scale Sensor Networks," *in Proc. IEEE MASS*, Oct. 2004.
[5] W. Wang, V. Srinivasan, K. C. Chua, and B. Wang, "Energy-efficient Coverage for Target Detection in Wireless Sensor Networks," *in Proc. IPSN*, Apr. 2007.
[6] J. Zhang, T. Yan, and S. Son, "Deployment Strategies for Differentiated Detection in Wireless Sensor Networks," *in Proc. IEEE SECON*, 2006.
[7] T.-L. Chin, P. Ramanathan, and K. K. Saluja, "Analytical Modeling of Detection Lantency in Mobile Sensor Networks," *in Proc. IPSN*, 2006.
[8] T. Clouqueur, K. K. Saluja, and P. Ramanathan, "Fault Tolerance in Collaborative Sensor Networks for Target Detection," *IEEE Transactions on Computers*, vol. 53, no. 3, pp. 320–333, 2004.
[9] P. Varshney, *Distributed Detection and Data Fusion*. Springer, 1997.
[10] R. Viswanathan and P. Varshney, "Distributed Detection with Multiple Sensors I. Fundamentals," *in Proc. the IEEE*, vol. 85, no. 1, 1997.
[11] R. Blum, S. Kassam, and H. Poor, "Distributed Detection with Multiple Sensors I. Advanced Topics," *in Proc. the IEEE*, vol. 85, no. 1, 1997.
[12] M. D. X. Luo and Y. Huang, "On Distributed Fault-tolerant Detection in Wireless Sensor Networks," *IEEE Transactions on Computers*, vol. 55, no. 1, pp. 58–70, 2006.
[13] L. Yu, L. Yuan, G. Qu, and A. Ephremides, "Energy-driven Detection Scheme with Guaranteed Accuracy," *in Proc. IPSN*, Apr. 2006.
[14] M. Duarte and Y. Hu, "Distance Based Decision Fusion in a Distributed Wireless Sensor Network," *in Proc. IPSN*, Apr. 2003.
[15] E. L. N. Katenka and G. Michailidis, "Local Vote Decision Fusion for Target Detection in Wireless Sensor Networks," Univ. of Michigan, Dept. of Statistics, Technical report, 2006.
[16] B. Liu, P. Brass, O. Dousse, P. Nain, and D. Towsley, "Mobility Improves Coverage of Sensor Networks," *in Proc. ACM MobiHoc*, May 2005.
[17] L. Wang and S. S. Kulkarni, "Sacrificing a Little Coverage Can Substantially Increase Network Lifetime," *in Proc. IEEE SECON*, Sept. 2006.
[18] S. Meguerdichian, F. Koushanfar, G. Qu, and M. Potkonjak, "Exposure In Wireless Ad-Hoc Sensor Networks," *in Proc. ACM MobiCom*, 2001.
[19] S. Aldosari and J. Moura, "Fusion in Sensor Networks with Communication Constraints," *in Proc. IPSN*, Apr. 2004.
[20] J.-J. Xiao, S. Cui, Z.-Q. Luo, and A. Goldsmith, "Joint Estimation in Sensor Networks under Energy Constraints," *in IEEE SECON*, 2004.
[21] F. Zhao, J. Liu, J. Liu, L. J. Guibas, and J. Reich, "Collaborative signal and information processing: an information-directed approach," *in Proc. the IEEE*, vol. 91, no. 8, pp. 1199–1209, Aug. 2003.
[22] J. Singh, U. Madhow, R. Kumar, S. Suri, and R. Cagley, "Tracking Multiple Targets Using Binary Proximity Sensors," *in Proc. IPSN*, 2007.
[23] A. D'Costa and A. Sayeed, "Collaborative Signal Processing for Distributed Classification in Sensor Networks," *in Proc. IPSN*, Apr. 2003.
[24] A. Arora, P. Dutta, S. Bapat, V. Kulathumani, H. Zhang, V. Naik, V. Mittal, H. Cao, M. Demirbas, M. Gouda, Y. Choi, T. Herman, S. Kulkarni, U. Arumugam, M. Nesterenko, A. Vora, and M. Miyashita, "A Lin in the Sand: a Wireless Sensor Network for Target Detection, Classification, and Tracking," *in Computer Networks (Elsevier)*, vol. 46, no. 5, pp. 605–634, Dec. 2004.
[25] F. Ye, H. Luo, J. Cheng, S. Lu, and L. Zhang, "A Two-tier Data Dissemination Model for Large-scale Wireless Sensor Networks," *in Proc. ACM MobiCom*, Sept. 2002.
[26] C. Gui and P. Mohapatra, "Power Conservation and Quality of Surveillance in Target Tracking Sensor Networks," *in ACM MobiCom*, 2004.
[27] J. W. Hui, Z. Ren, and B. Krogh, "Sentry-based Power Management in Wireless Sensor Networks," *in Proc. IPSN*, Apr. 2003.
[28] L. Gu and J. Stankovic, "Radio-Triggered Wake-Up Capability for Sensor Networks," *in Proc. IEEE RTAS*, Apr. 2004.
[29] S. C. Port, *Theoretical Probability for Applications*. John Wiley & Sons, 1994.
[30] P. Hall, *Introduction to the Theory of Coverage Process*. John Wiley & Sons, 1988.
[31] G. Yang, V. Shukla, and D. Qiao, "A novel on-demand framework for collaborative objection detection in sensor networks," *in Proc. IEEE Infocom Mini-conference*, 2008.